

# Coordinating Microscopic Robots in Viscous Fluids\*

Tad Hogg  
HP Labs  
Palo Alto, CA

October 9, 2006

## Abstract

Multiagent control provides strategies for aggregating microscopic robots (“nanorobots”) in fluid environments relevant for medical applications. Unlike larger robots, viscous forces and Brownian motion dominate the behavior. Examples range from modified microorganisms (programmable bacteria) to future robots using ongoing developments in molecular computation, sensors and motors. We evaluate controls for locating a cell-sized area emitting a chemical into a moving fluid with parameters corresponding to chemicals released in response to injury or infection in small blood vessels. These control methods are passive Brownian motion, following the chemical concentration gradient, and cooperative behaviors in which some robots use acoustic signals to guide others to the chemical source. Control performance is evaluated using diffusion equations to describe the robot motions and control state transitions. The quantitative results show these control techniques are feasible approaches to the task with trade-offs among fabrication difficulty, response speed, false positive detection rate and energy use. Controlled aggregation at chemically distinctive locations could be useful for sensitive diagnosis, selective changes to biological tissues and forming structures using previous proposals for multiagent control of modular robots.

keywords: multiagent robot control design, nanomedicine, nanotechnology

## 1 Microscopic Robots

Robots with sizes comparable to bacteria (“nanorobots”) could provide many novel capabilities through their ability to sense and act in microscopic environments. Microscopic robots could be useful in a wide variety of biological research and medical contexts. For instance, robots and nanoscale-structured materials inside the body could significantly improve disease diagnosis and treatment [23, 45, 46, 39].

Realizing these benefits requires fabricating robots cheaply, in large numbers and with suitable physical and computational capabilities. Such fabrication is beyond the ability of current technology. Nevertheless, current progress in engineering nanoscale devices could eventually enable production of such robots. For example, ongoing development [16, 17, 34, 25, 44, 55] of molecular-scale electronics, sensors and motors provides components for such robots, though these cannot yet be assembled into large numbers of complete systems. Demonstrations of programmable bacteria [59, 60] produce large numbers of microscopic systems with simple programmed control, and DNA computers can respond to logical combinations of specific chemicals in their environment [4]. However biological organisms have restricted material properties and, by using protein synthesis to perform logic operations, severely limited computational complexity and speed for control programs.

Beyond the challenge of fabricating the robots is designing controls for their physical environments, tasks and capabilities, which differ considerably from those of larger robots. Fortunately, we can evaluate control methods prior to building the robots via simulation using plausible robot capabilities and task environments [20, 23, 50]. Moreover, suitable control can compensate for some hardware limitations (e.g., limited locomotion ability or sensor accuracy). Thus studies of control approaches can identify useful tasks for robots with limited hardware capabilities. More generally, computational studies of controlling groups

---

\*to appear in *Autonomous Agents and Multi-Agent Systems*

of robots complement those of individual nanoscale devices [42, 58], thereby developing systems architectures for microscopic robots. Identifying combinations of robot capabilities sufficient for various tasks also motivates developing the required fabrication technologies.

Robots could act independently, e.g., when detecting specific patterns of chemicals, in analogy to swarms [8] used in foraging, surveillance or search tasks. In this case, new applications arise mainly from the *in vivo* access microscopic robots have to small sizes (e.g., individual cells), and their large numbers. Of more interest for multiagent systems are tasks requiring coordinated behavior among the robots. One example is responding to an injury or infection site, in which many robots must aggregate to the site, but not so many as to interfere with other processes (e.g., by fully blocking blood vessels). Such aggregation could be necessary to mount an adequate rapid response to infection or, more ambitiously, to have the robots form structures, e.g., to temporarily close tears in blood vessels or act as scaffolding to enhance tissue repair. Thus, locating chemically distinctive microscopic sites is a basic task for these robots.

A direct approach to aggregation is simply to place the robots at the desired location, e.g., for microsurgery at specific, well-localized sites. Such robots could provide sensing and actuation capabilities at cellular length scales, e.g., for repairing injured nerves [32]. In other situations, the existence of a target, let alone its precise location, may not be known *a priori*. Instead targets, such as infecting bacteria, may only have a functional specification, with at best only coarse knowledge of their location. In that case the robots would need to find the target. With a sufficient number of robots circulating in the bloodstream, some will pass near any given location frequently. Their challenge is to recognize a target area matching a preprogrammed specification, and respond, as they pass by. With communication, robots near the target could help others find it, either directly or via environmental modification, i.e., stigmergy [8]. Aggregating microscopic robots differs significantly from larger robots [41] in several respects. First the physical environment is dominated by viscous fluid flow and requires motion in three dimensions. Second, thermal noise is significant for sensors and Brownian motion limits the ability to follow precisely specified paths. Third, targets are recognizable via chemical signatures rather than, say, visual markings or specific shapes. Fourth, the tasks involve large numbers of robots, each with limited capabilities in sensing, actuation, communication and computation. These features suggest reactive multiagent control is particularly well-suited for microscopic robots.

Among the many open issues for system architecture design, this paper focuses on controls suitable for the transition from independent to aggregated behaviors at chemically distinctive locations. This paper examines the feasibility of simple multiagent control for aggregation at a target location marked by a chemical signal. The emphasis here is on feasible response with plausible biophysical parameters and robot capabilities. These feasible controls could form the basis of more elaborate tasks for which aggregation is one component. Future studies could also optimize the controls for various tasks. Relevant optimality criteria include minimizing hardware capabilities to simplify fabrication, enhancing measurement accuracy for biological research, and optimizing safety, speed and accuracy for treatment in a clinical setting. The last case would emphasize both good performance in the targeted situation and a sufficiently low false positive rate to avoid detrimental actions.

The physical parameters for the task scenario studied here arise from the initial immunological response to a minor infection or injury. In this process, the injured area produces chemical signals which enter nearby small blood vessels to recruit white blood cells [36]. Compared to the immune response, the robots could detect the signals and initiate response more rapidly [11]. They could also identify the cause of the signal (e.g., a type of infecting bacteria) and, unlike cells, communicate that information to the attending physician [23], providing earlier and more accurate diagnosis. Finally, the robots could aid in treatment, e.g., by delivering drugs only to cells matching a prespecified chemical profile [23] as an extension of a recent *in vitro* demonstration of this capability using DNA computers [4].

The remainder of this paper first describes approaches to evaluating microscopic robot behaviors and the aggregation task, emphasizing physical properties differing significantly from those of larger robots. The following sections describe the main physics relevant for the robots, several control strategies and the resulting behaviors.

## 2 Evaluating Robot Control Methods

Computational studies of robots involve trade-offs among accuracy of modeling individual robots and their environment, the number of robots and computational cost. The same issues arise with microscopic robots, with the additional difficulty of not yet having physical experiments for validation. Nevertheless observed behaviors of microorganisms, which face the same physical constraints as future microscopic robots, give some guidelines for feasible behaviors.

One approach to investigate microscopic robots focuses on collective behaviors in a highly simplified environment, such as cellular automata. For example, a two-dimensional scenario shows how robots could assemble structures [3] from local rules, but does not include physical behaviors such as fluid flow. Distributed controls for swarms [8] are likely to be well-suited to microscopic robots with their limited physical and computational capabilities and large numbers. Most such studies focus on macroscopic robots or behaviors in abstract spaces [28] which do not specifically include physical properties unique to microscopic robots. In spite of the simplified physics, these studies show how local interactions among robots lead to various collective behaviors.

Simulations including physical properties of microscopic robots and their environments give more accurate robot performance. Such studies identify feasible tasks for robots with various capabilities using a range of assumptions about the task environment. Examining a range of plausible scenarios is important because quantitative physical properties of interesting microenvironments are not precisely known so simulations necessarily use rough estimates. Simpler models, such as a two-dimensional simulation of chemotaxis [18], provide insight into robot capabilities useful for finding microscopic chemical sources. A more elaborate simulator [14, 13] includes three-dimensional motions in viscous fluids, Brownian motion and environments with numerous cell-sized objects, though without accounting for how they change the fluid flow. This simulation uses a threshold distance for detecting chemical signals rather than diffusion in the moving fluid and so has not examined signal-to-noise limitations from low concentrations or shallow gradients of the target chemical.

A third approach to robot behaviors employs a stochastic mathematical framework for distributed computational systems [31, 40]. This method directly evaluates the average behaviors of many robots, which would otherwise need numerous repeated runs of a simulation. This approach is best suited for simple control strategies, with minimal dependencies on events in individual robot histories. Microscopic robots, with limited computational capabilities, are likely to be used with relatively simple reactive controls for which this analytic approach is ideally suited. As one example, the analysis has been applied to following chemical gradients in a one-dimensional geometry without fluid flow [27]. While this study ignores much of the significant physics of microscopic fluid environments and sensor noise, it extends this analysis technique to the case of spatially varying fields. Spatial fields, such as fluid velocity and chemical concentrations, are particularly relevant for microscopic robots.

Cellular automata, swarms, physically-based simulations and stochastic analysis are all useful tools for evaluating the behaviors of microscopic robots. For operating in fluids, these approaches have not yet addressed a number of significant questions, such as the feasibility of rapid, fine-scale response to chemical events too small for detection with conventional approaches. Nor have prior studies addressed controls suited to various plausible combinations of robot capabilities, particularly including sensor noise inherent in the discrete molecular nature of low concentrations. For instance, in contrast to assuming robots can rapidly and accurately determine concentration gradients, noise is significant for robots moving in a fluid with the need to balance the long time required to collect adequate statistics with the short time available to respond before the fluid flow moves the robot well past the target. Finally, prior studies of how well microscopic robots find chemical sources have not considered false positives: spurious detections due to statistical fluctuations from the background concentration of the chemical. Although such detections can be rare, when applied to tasks involving small targets in a large tissue volume, the number of opportunities for false positive responses can be orders of magnitude larger than the opportunities for true positive detections of a target. Thus even a low false positive rate can lead to many more false positive detections than true target detections.

This paper examines these issues in a prototypical task to identify performance of various control choices. We use the stochastic analysis approach. This allows incorporating more realistic physics than used with cellular automata studies, and is computationally simpler than repeated simulations to obtain average behaviors. This technique is limited in requiring approximations for dependencies introduced by the robot history, but

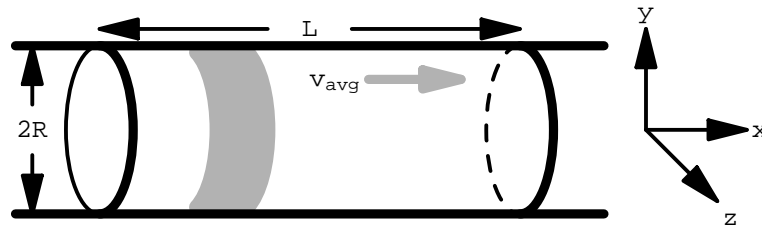


Figure 1: Schematic illustration of the task geometry as a section, of length  $L$ , of a longer pipe, with radius  $R$ . Fluid flows in the positive  $x$ -direction with average velocity  $v_{avg}$ . The gray area is the target region on the surface of the pipe.

readily incorporates physically realistic models of sensor noise and consequent mistakes in the robot control decisions. The stochastic analysis indicates the plausible range of performance of various control methods, on average, and thereby suggests scenarios suited for further, more detailed, simulation studies. The results also provide useful validation test cases for such simulations. Finally, the results suggest opportunities for improved performance by more elaborate multiagent control methods.

### 3 Finding a Cell-Sized Chemical Source

The microenvironments of the circulatory system vary considerably in size, flow rates, and other physical properties. Moreover, chemicals in the blood have a range of concentrations, diffusion coefficients, and sources. As a challenging scenario, we consider a chemical released from an area about equal to that of a single cell lining a blood vessel. This allows examining the feasibility of finding an infection while still extremely small, and hence unlikely to be noticeable by larger-scale conventional diagnostic tools much less provide any noticeable symptoms. The task is a simplified version of finding a single chemically distinctive cell within the body, assuming it produces chemicals that diffuse into only one tiny blood vessel. In practice, infections or injuries generally involve a large number of cells and chemicals introduced in many nearby vessels making the search easier than the task considered here.

For an initial study of this task, we consider a vessel containing only flowing fluid, robots spaced far apart compared to their size and a diffusing chemical arising from a target area on the vessel wall. This scenario produces a static concentration of the chemical signal throughout the vessel, thereby simplifying the analysis. The robots, with sensors for this chemical, must find the source on the vessel wall. We suppose the target has distinctive chemical properties, e.g., chemical receptors allowing the robots to detect it when they physically are in contact with the target area. We examine the rate at which robots find the target, the energy they use and the false positive rate.

Table 1 lists the physical parameters involved in this task. Small vessels have diameters up to several tens of microns, and lengths of about a millimeter. We focus on a short segment in the middle of such a vessel to avoid considering fluid dynamics from vessel branching at the ends. Fig. 1 shows the geometry of our task: a segment of the vessel of length  $L$  with a target region on the wall emitting a chemical into the fluid. Robots continually enter one end of the vessel with the fluid flow.

The robot density corresponds to  $10^{12}$  robots in the entire 5-liter blood volume of a typical adult, an example of medical applications using a huge number of microscopic robots [23]. In spite of this large number, the robots use only about  $10^{-3}$  of the vessel volume, far less than the 20% – 40% occupied by blood cells. The total mass of all the robots is about 4g. For simplicity, we consider spherical robots.

For chemical detection, we consider a typical protein produced in response to injury, with concentration near the injured tissue of about 30ng/ml and background concentration in the bloodstream about 300 times smaller. These chemicals, called chemokines, are proteins with molecular weight around  $10^4$  daltons. These values lead to the parameters for the chemical given in Table 1.

parameter	value
<b>vessel and target</b>	
vessel radius	$R = 5\mu\text{m}$
section length	$L = 100\mu\text{m}$
target length	$L_{\text{target}} = 30\mu\text{m}$
<b>fluid</b>	
fluid density	$\rho = 1\text{g}/\text{cm}^3$
fluid viscosity	$\eta = 10^{-2}\text{g}/\text{cm}\cdot\text{s}$
average fluid velocity	$v_{\text{avg}} = 1000\mu\text{m}/\text{s}$
fluid temperature	$T = 310\text{K}$
<b>robots</b>	
robot radius	$a = 1\mu\text{m}$
number density of robots	$\rho_{\text{robot}} = 2 \times 10^{-4} \text{ robot}/(\mu\text{m})^3$
robot diffusion coefficient	$D_{\text{robot}} = 0.076 \mu\text{m}^2/\text{s}$
<b>chemical signal</b>	
production flux at target	$F_{\text{target}} = 56 \text{ molecule}/\text{s}/(\mu\text{m})^2$
diffusion coefficient	$D = 100\mu\text{m}^2/\text{s}$
concentration near source	$1.8 \text{ molecule}/(\mu\text{m})^3$
background concentration	$6 \times 10^{-3} \text{ molecule}/(\mu\text{m})^3$
<b>acoustic signal</b>	
speed of sound	$v_{\text{sound}} = 1.5 \times 10^9 \mu\text{m}/\text{s}$

Table 1: Parameters for the environment, robots and the chemical signal used in our task. The robots are spheres with radius  $a$ . The chemical signal concentrations represent a typical 10 kilodalton chemokine molecule, with mass concentrations near the source and background (i.e., far from the source) equal to  $3 \times 10^{-8}\text{g}/\text{ml}$  and  $10^{-10}\text{g}/\text{ml}$ , respectively.

We suppose the target region produces the chemical uniformly with flux  $F_{\text{target}}$ . Total target surface area is  $2\pi RL_{\text{target}} \approx 940\mu\text{m}^2$ , about the same as the surface area of a single endothelial cell lining a blood vessel. Thus the value for  $F_{\text{target}}$  in Table 1 corresponds to  $5 \times 10^4 \text{ molecule}/\text{s}$  from the target area as a whole. This flux makes the concentration at the target region equal to that given in Table 1.

To examine the rate of false positives, we consider a scenario in which robots can be coarsely localized to a region of interest, say over a range of 1cm or so. Robots moving with flow will thus have this relatively large distance to move in regions containing only the background concentration, providing numerous opportunities for incorrectly interpreting background concentration as target signals. Prior knowledge of the relevant concentrations allows setting control decision thresholds to balance the likelihood of correctly detecting the target with the chance for false positives, as described below in the discussion of specific control methods.

## 4 Physics of Fluid Microenvironments

The physics of microscopic objects moving in fluids is a key difference between microscopic robots and larger ones. This section highlights the key physical properties of robot motion and chemical diffusion relevant for the robot task examined here.

### 4.1 Fluid Motion

Viscosity dominates the robot motion through the fluid, with different physical behaviors than our experience with larger organisms and robots [48, 57, 26, 37]. The ratio of inertial to viscous forces for an object of size  $s$  moving with velocity  $v$  through a fluid with viscosity  $\eta$  and density  $\rho$  is given by the Reynolds number  $\text{Re} \equiv s\rho v/\eta$ . Using typical values for density and viscosity (e.g., of water or blood plasma) in Table 1 and noting that reasonable speeds for robots with respect to the fluid [23] are comparable to the fluid flow speed in small vessels, i.e.,  $\sim 1\text{mm}/\text{s}$ , motion of a 1-micron robot has  $\text{Re} \approx 10^{-3}$ , so viscous forces dominate.

Consequently, robots applying a locomotive force quickly reach terminal velocity in the fluid, i.e., applied force is proportional to velocity rather than the more familiar proportionality to acceleration of Newton's law  $F = ma$ .

Flow in a pipe of uniform diameter has a parabolic velocity profile, i.e., the velocity at distance  $r$  from axis is

$$v(r) = 2v_{\text{avg}}(1 - (r/R)^2) \quad (1)$$

where  $v_{\text{avg}}$  is the average speed at which fluid moves through the pipe. Objects, such as the robots, moving in the fluid alter the velocity profile of the fluid to some extent. For simplicity, and due to the relatively small volume of the vessel occupied by the robots, we ignore these changes and treat the fluid flow profile as constant in time and given by Eq. (1).

## 4.2 Drag on Objects Moving in the Fluid

Robots moving through the fluid encounter significant drag. For instance, the drag force on an isolated sphere is

$$6\pi a\eta v \quad (2)$$

for radius  $a$ , fluid viscosity  $\eta$  and speed  $v$  with respect to the fluid. Although not quantitatively accurate near boundaries or other objects, this expression gives a rough estimate of the drag in those cases as well. For instance, a numerical evaluation of drag force on a  $1\mu\text{m}$ -radius sphere moving at velocity  $v$  with respect to the fluid flow near the center of a  $5\mu\text{m}$ -radius pipe, has drag about three times larger than given by Eq. (2). In terms of evaluating power requirements, such modest factors can be included in the locomotion efficiency.

Due to fluid drag and the inefficiencies of locomotion in viscous fluids, robots moving through the fluid at  $\approx 1\text{mm/s}$  dissipate a picowatt [5]. Thus, if all the robots moved simultaneously they would use about one watt, compared to a typical person's 100-watt resting power consumption.

Fluid drag moves robots with the fluid. As an approximation, we assume robots without active locomotion move with the same velocity as fluid would have at the center of the robot if the robot were not there. Numerical evaluation of the fluid forces on the robots for the parameters of Table 1 show the robots indeed move close to this speed when the spacing between robots is many times their size.

## 4.3 Diffusion of Robots and Chemicals

Diffusion arising from Brownian motion is important for microscopic robots, and even more so for the chemical molecules. The diffusion coefficient  $D$ , depending on an object's size, characterizes the resulting random motion, with root-mean-square displacement of  $\sqrt{6Dt}$  in a time  $t$ . For the parameters of Table 1, this displacement for the robots is about  $0.7\sqrt{t}$  microns with  $t$  measured in seconds. Brownian motion also randomly alters robot orientation.

The target chemical has much larger concentration and diffusion coefficient than robots, as indicated in Table 1. Quantitatively, the chemical concentration  $C$  is governed by the diffusion equation [5]

$$\frac{\partial C}{\partial t} = -\nabla \cdot \mathbf{F} \quad (3)$$

where  $\mathbf{F} = -D\nabla C + \mathbf{v}C$  is the chemical flux, i.e., the rate at which molecules pass through a unit area, and  $\mathbf{v}$  is the fluid velocity vector. The first term in the flux is diffusion, which acts to reduce concentration gradients, and the second term is motion of the chemical with the fluid.

With nonuniform velocity, e.g., that of Eq. (1), Eq. (3) lacks a simple analytic solution so must be solved numerically. At the target, the flux into the vessel,  $F_{\text{target}}$ , produces the measured concentration of signal near the source, described in Table 1.

Fig. 2 shows the resulting steady-state concentration, which decreases with distance from the target. We also see the high concentration contours are pushed downstream by the fluid flow. Thus robots monitoring for the chemical signal from the target area are unlikely to detect the signal until they are downstream of the target. As a check on the sufficiency of the vessel length considered here, solving Eq. (3) for a  $200\mu\text{m}$  section, gave no significant change in the concentrations shown in Fig. 2.

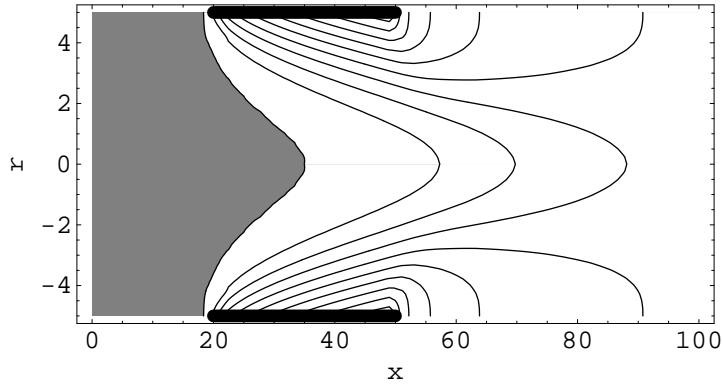


Figure 2: Concentration contours on a cross section through the vessel, including the axis ( $r = 0$ ) in the middle and the walls ( $r = \pm R$ ) at the top and bottom. The gray area shows the region where the concentration from the target is below that of the background concentration. The thick black lines along the vessel wall mark the extent of the target region. The vertical and horizontal scales are different: the cross section is  $10\mu\text{m}$  vertically and  $100\mu\text{m}$  horizontally. Numbers along the axes denote distances in microns.

## 5 Sensors for Microscopic Robots

Current robots often use sonar or cameras to sense their environment. These sensors locate objects from a distance, and involve sophisticated interpretation algorithms with extensive computational requirements. In contrast, microscopic robots for biological applications will mainly rely on chemical sensing, using receptors designed to detect specific chemicals. In this case, relatively simple pattern recognition algorithms should suffice to interpret the sensor data, thereby allowing molecular computers with modest capabilities to provide the necessary computations. However, statistical noise is a significant limitation on the accuracy of sensors for microscopic robots. This section provides estimates of the signal-to-noise ratio for sensing the chemical from the target and acoustic signals from other robots. The robot capabilities considered here use plausible engineering parameters for molecular scale devices such as molecular electronics [58] and nanoscale sensors [47, 54].

### 5.1 Chemical Detection

Microscopic robots and bacteria face similar physical constraints in detecting chemicals [6]. At the concentrations of Table 1 robots encounter only a few molecules of the chemical as they pass the target. Current nanoscale chemical sensors are effective at concentrations well below those of Table 1 and performance at these concentrations is primarily limited by the time required for molecules to reach the sensor [47, 54]. Thus statistical fluctuations in the number encountered is the dominant source of sensor noise for the task considered here.

At the sizes of these robots, chemical diffusion is rapid enough to allow sensors covering a small fraction of the robot surface to have detection efficiency close to that obtained with the entire robot surface covered with sensors [5]. Thus as a simple analysis of sensor capability we consider a robot whose entire surface can absorb and recognize the particular signal molecule from the target.

The diffusive capture rate  $\alpha$  for a sphere of radius  $a$  in a region with concentration  $C$  is [5]

$$\alpha = 4\pi DaC \quad (4)$$

Using Table 1,  $\alpha \approx 7.6$  molecule/s at the background concentration and  $\approx 2300$  near the target. Detection over a time interval  $\Delta t$  is a Poisson process with mean value  $\alpha\Delta t$ .

A robot encounters changing concentrations as it moves. The expected number of sensor counts a robot

at position  $\mathbf{r}$  has received from the target chemical during a prior measurement interval time  $T_{\text{measure}}$  is

$$K(\mathbf{r}) = 4\pi Da \int_0^{T_{\text{measure}}} C(\mathbf{r}'(\mathbf{r}, \tau)) d\tau \quad (5)$$

where  $\mathbf{r}'(\mathbf{r}, \tau)$  denotes the location the robot had at time  $\tau$  in the past. During the time the robot passes the target, Brownian motion displacement is  $\sim 0.1\mu\text{m}$ , which is small compared to the  $10\mu\text{m}$  vessel diameter. Thus the possible past locations leading to  $\mathbf{r}$  are closely clustered and for estimating the number of molecules detected while passing the target, a reasonable approximation is the robot moves deterministically with the fluid. In our axially symmetric geometry with fluid speed given by Eq. (1), positions are specified by two coordinates  $\mathbf{r} = (r, x)$  so  $\mathbf{r}'((r, x), \tau) = (r, x - v(r)\tau)$  when the robot moves passively with the fluid and Brownian motion is ignored. During this motion, the robot will, on average, also encounter

$$k = 4\pi DacT_{\text{measure}} \quad (6)$$

molecules from the background concentration, not associated with the target.

The values  $K$  and  $k$  are average counts of a Poisson process: the expected number of counts when a signal is present is  $K + k$ , and  $k$  when there is no signal. Reliably distinguishing these cases requires the difference in these values to be large compared to the standard deviation, i.e., the signal-to-noise ratio for detecting the chemical from the target is  $SN = K/\sqrt{K + k}$ .

The choice of measurement time must balance having enough time to receive adequate counts, thereby reduce errors due to statistical fluctuations, while still responding before the robot has moved far downstream of the target where response would require moving upstream against the fluid flow. Moreover, far downstream of the target the concentration from the target is small so additional measurement time is less useful. To decide when a signal from the target is present, the robot can use a threshold value of the counts  $C_{\text{threshold}}$ , i.e., considering a signal detected when the sensor counts over the measurement time reach or exceed this value. A low value for  $C_{\text{threshold}}$  will produce many false positives, while a high value means many robots will pass the target without detecting it (i.e., false negatives).

With these control parameters we can determine the rate at which a robot detects a signal. Consider a robot at  $\mathbf{r}$ . During a small time interval  $\Delta t$  the probability to detect a molecule is  $4\pi Da(C(\mathbf{r}) + c)\Delta t \ll 1$ . For a robot to first conclude it has detected a signal during this short time it must have  $C_{\text{threshold}} - 1$  counts in the prior  $T_{\text{measure}}$  time interval and then one additional count during  $\Delta t$ . Thus the rate at which robots first conclude they detect a signal is

$$4\pi Da(C + c) \frac{\text{Po}(K + k, C_{\text{threshold}} - 1)}{\sum_{n < C_{\text{threshold}}} \text{Po}(K + k, n)} \quad (7)$$

where  $\text{Po}(\mu, n) = e^{-\mu}\mu^n/n!$  is the Poisson distribution. In Eq. (7)  $C$  and  $K$  depend on robot position and the last factor is the probability the robot has  $C_{\text{threshold}} - 1$  counts in its measurement time interval, given it has not already detected the signal, i.e., the number of counts is less than  $C_{\text{threshold}}$ . Eq. (7) also gives the detection rate when there is no target, i.e., false positives, by setting  $C$  and  $K$  to zero.

## 5.2 Chemical Gradient Detection

After detecting a signal, a robot could use the concentration gradient to determine direction to move. The gradient signal, involving the difference between measurements, is harder to detect than just the presence of the chemical. As with bacteria, two strategies for gradient detection [22] are in space, by comparing counts at different parts of the robot at the same time, and in time, by moving a bit through the fluid and comparing counts received by the entire surface of the robot at different times. The temporal approach involves moving for various times, with random changes in direction based on how much chemical is detected. Bacteria use this temporal technique of chemotaxis [1, 6, 21].

For the robot size we consider, these two approaches to gradient estimation have similar performance [22]. For simpler analysis, we consider the spatial method. An estimate of time required to determine the gradient [6, 21] is a signal-to-noise ratio greater than 1 for the difference in concentration between two sides of a spherical absorber. In our case, this measurement takes place while the robot is moving with the fluid.

The expected gradient signal measured for time  $T_{\text{measure}}$  is the difference in numbers for the two sides of the robot, each determined with Eq. (5), to give a signal of  $S = (a/2)K/\gamma$  where  $\gamma = K/|\nabla K|$  characterizes the distance over which the measured concentration changes significantly. The background concentration does not contribute to the gradient signal. This expression assumes the robot size is small compared to  $\gamma$ . For larger gradients, i.e., very near the target, the signal can be estimated instead from the difference in the  $K$  values from Eq. (5) for the two sides of the robot. The variance in counts includes both the signal from target and background concentration, so signal-to-noise ratio for estimating the gradient is

$$\frac{S}{\sqrt{K+k}} \quad (8)$$

Brownian motion limits the time available for gradient estimation. For a  $1\mu\text{m}$  sphere in water, the orientation changes by one radian in about three seconds. Thus, unless the robot rigidly attaches itself to the vessel wall or has other reference points to maintain its orientation, it must estimate the gradient by comparing signal on opposite sides well within this time to accumulate counts from substantially the same directions. In our case, the motion with the fluid provides a more severe constraint to estimate gradient before the robot has moved far downstream of the target. With the parameters of Table 1 we find reasonable signal-to-noise near the target even with measurement time as short as 10ms, well within the Brownian motion limit and while the robot is still near the target.

### 5.3 Communication with Acoustic Signals

Robots can communicate to coordinate activities. For robots with chemical sensors, a natural communication mechanism is via chemical signals. However, while chemical signals could be useful to coordinate robots already at the target, they are not effective for communicating over distances beyond a few microns, especially to reach robots upstream from the target.

For longer range communication, acoustic signals allow communication well upstream of the target region. For instance, communicating between neighboring robots requires signals detectable over distances of about  $100\mu\text{m}$ , based on the density of robots given in Table 1. Such signals take about  $100\mu\text{m}/v_{\text{sound}} \sim 10^{-4}\text{ms}$  to reach the receiver. Compared to fluid flow and robot motion speeds, acoustic signals are essentially instantaneous.

Acoustic signal power decreases due to spreading, decreasing as the square of the distance from the source, and absorption, decreasing exponentially with distance. Absorption increases at higher frequencies. For communication distances relevant here, up to  $100\mu\text{m}$  or so, and frequencies up to 100MHz or so, absorption in water is at most a few percent, hence negligible compared to the decrease due to spreading. Thus a  $1\mu\text{m}$  robot radiating with power  $P$ , produces a signal with power  $10^{-4}P$  at distance  $100\mu\text{m}$ . Such a signal with bandwidth  $\nu$  can achieve a maximum communication rate [53] of  $\nu \log_2(1 + 10^{-4}P/(k_B T \nu))$ , where  $k_B$  is the Boltzmann constant. For instance, broadcasting at 100MHz with  $P = 10^4\text{pW}$  gives a maximum communication rate of  $\sim 170\text{MHz}$  to robots  $100\mu\text{m}$  away. Practical receivers will not achieve this maximum, but could get close. Thus, a robot could communicate  $\sim 10$  bits to other robots within  $100\mu\text{m}$  using energy of  $E_{\text{signal}} \approx 10^{-15}\text{J}$ . Communication over the diameter of the vessel, i.e.,  $\sim 10\mu\text{m}$ , requires 100 times less energy. The alert signals used with the control methods discussed in this paper in principle only need communicate a single bit so this value for  $E_{\text{signal}}$  allows some redundancy to ensure reliable communication.

The efficiency of converting mechanical motion to sound increases with frequency. A simple model of this conversion [23] arises from Eq. (2) when the robot is small compared to the wavelength, i.e., the frequency is small compared to  $v_{\text{sound}}/a = 1500\text{MHz}$ . For microscopic robots in water, efficiencies can exceed 50% at frequencies above 100MHz. Such sound production is far more efficient than converting mechanical motion into movement through the fluid.

### 5.4 Locating the Vessel Wall

With the target located on the vessel wall and slower fluid motion near the wall, moving to the walls can be a useful robot capability. One approach, requiring no sensing ability beyond recognizing the wall when the robot touches it, is random motion.

Faster response is possible if the robot can determine the direction to the wall. As one approach, acoustic echo location could detect walls in small vessels. Power requirements are less severe than for longer range communication discussed above. Spatial resolution is about  $v_{\text{sound}}/\nu$ , so using  $\nu = 1500\text{MHz}$  gives  $\sim 1\mu\text{m}$  resolution, comparable to the size of the robot

A second approach to determining the direction to the vessel wall is based on fluid flow. At low Reynolds number, boundary effects extend far into vessel, in particular giving higher fluid shear rates nearer the wall. Nanoscale sensors can measure fluid flow rates over speeds relevant for the task discussed here [29]. Several such sensors, extending a small distance from the robot surface in various directions could estimate shear rates and hence the direction to the wall.

## 5.5 Additional Robot Capabilities

The robots require additional capabilities than the sensors described above. For instance, robots may also detect signals broadcast from outside the body. Such signals could activate the robots only within certain areas of the body at, say, centimeter length scales.

Chemical signal detection using thresholds in a given time interval requires the robot to have a clock. This clock need not be globally synchronized with other robots, but should be able to measure millisecond time intervals. The robot could use the clocking pulses of its molecular electronic computational circuit which would likely operate at higher frequencies and thus readily provide millisecond timing as well. Acoustic communication, if used by the robots, would also involve much higher frequency oscillators than required for chemical signal timing.

Interpreting sensors and executing control programs also requires on-board computation. For the controls examined here, a robot must make decisions on millisecond time scales, involving at least a few arithmetic operations to compare sensor counts to specified thresholds stored in memory. As a minimum estimate on required computational capability, these operations amount to around 100 elementary logic operations and memory bit accesses within a 10ms measurement and response time. This gives about  $10^4$  logic operations per second. While modest compared to current computers, this rate is significantly faster than demonstrated use of programmable bacteria [59, 60].

This computation rate requires energy. Specifically, each logic operation in current electronic circuits use  $10^4 - 10^5$  times the thermal noise level  $k_B T = 4 \times 10^{-21}\text{J}$  at the fluid temperature of Table 1. Near term molecular electronics could reduce this to  $\approx 10^3 k_B T$ , in which case the required  $10^4$  operations per second uses a bit less than 0.1pW. This power is substantially below the power used for locomotion or communication in the control methods described below. However, those control actions will operate only occasionally, and for short times, when the robot detects a signal, whereas computation could be used continuously by robots monitoring for such signals. Additional energy will be needed for communication within the robot's computer and its memory.

The robots require power for operation. For tasks of limited duration, robots could be fabricated with an on-board fuel source. Alternatively, though likely requiring more difficult fabrication, the robots could use energy sources available in their environment. For instance, typical concentrations of glucose and oxygen in the bloodstream could generate  $\approx 1000\text{pW}$  continuously, limited primarily by the diffusion rate of the molecules to the robot [23]. Such energy sources could also provide higher bursts of power. Power is a constraint on control methods, particularly if fabrication technologies can only produce low efficiency devices. Limits on power use are also important for safety to avoid thermal damage to nearby biological tissues, particularly when robots aggregate.

## 6 Robot Control Techniques

We examine several control techniques. First, as a point of comparison, the robots use small Brownian motions to find the target by random search. In a second method, the robots monitor for chemical concentration significantly above the background level. After detecting a signal, the robot estimates the concentration gradient and moves toward higher concentrations. In these cases, robots find the target independently. In the third technique robots emit acoustic signals to aid others in finding the target. We examine two such communication protocols.

parameter	value
chemical measurement time	$T_{\text{measure}} = 10\text{ms}$
count threshold for signal detection	$C_{\text{threshold}} = 2$
robot locomotion speed	$v_0 = 1000\mu\text{m/s}$
reset time	$T_{\text{reset}} = 100\text{ms}$
<b>follow gradient</b>	
minimum signal-to-noise for gradient	$\text{SN}_{\text{min}} = 1$
<b>communication</b>	
energy for long-range acoustic signal	$E_{\text{signal}} = 10^{-15}\text{J}$
random motion time	$T_{\text{random}} = 1\text{ms}$
rate of signals from guides	$\omega = 100/\text{s}$
rate guides start searching	$\alpha_{\text{g}\rightarrow\text{w}} = 10/\text{s}$

Table 2: Control parameters.

In summary, we consider the following control methods:

- *random*: robots move passively with the fluid and reach the target only if they bump into it
- *follow gradient*: robots monitor for high signal concentration and, when detected, measure and follow the concentration gradient until reaching the target
- *communication*: robots detecting the chemical use acoustic signals to alert other robots to the presence of the target which then have one of two behaviors:
  - alerted robots move to the wall and then to the target
  - alerted robots move to the wall, temporarily act as guides for others using low-power communication, and then move to the target

We suppose robots reaching the target are removed from further consideration (e.g., they leave the vessel or release a chemical load and then become inactive). Thus in the equations describing the robot concentrations given below we simply treat the target area as capturing robots through the choice of boundary condition [5].

Due to statistical fluctuations in the chemical sensor counts, robots will occasionally mistake background concentration for a signal from the target. Since we consider an extreme case of the robots looking for one small target, the huge number of locations *without* the target could lead many robots to respond to false positives even with a relatively low rate of false positive detection. Thus the robot control programs described below include decisions to reset to the default MONITOR state when, after detecting a signal, further activities neither lead to the target nor continue to detect the signal after a specified time interval.

The remainder of this section describes the robot control program states and the transitions among them based on sensor events. These state diagrams lead directly to equations describing the average robot behaviors. We characterize robots positions by the locations of their centers, so a distance  $a$  from the vessel wall corresponds to a robot just touching the wall. We examine average behavior in terms of robot concentrations, i.e., average number of robots in each control state per unit volume, rather than conducting many simulation trials of motions of individual robots. The robot concentration is governed by a diffusion equation, similar to Eq. (3), with velocity given by a combination of fluid flow and any additional directed motions of the robot. Diffusion for the robots includes both Brownian motion and an additional contribution from any random motion deliberately performed by the robot or due to sensor noise. Boundary conditions for the diffusion equations have robots sticking to the target area once they find it and new robots entering the vessel segment with the fluid flow. This approach [40] gives aggregate behaviors, but does not follow individual robot histories or provide information on extreme, rather than average, behaviors. Thus this analysis approach complements simulation studies which can incorporate more detailed robot behavior, but must be run repeatedly to obtain average behaviors.

The control algorithms involve parameters listed in Table 2. These values are reasonable choices corresponding to the physical size of the target, fluid flow rate and chemical concentration, though are not

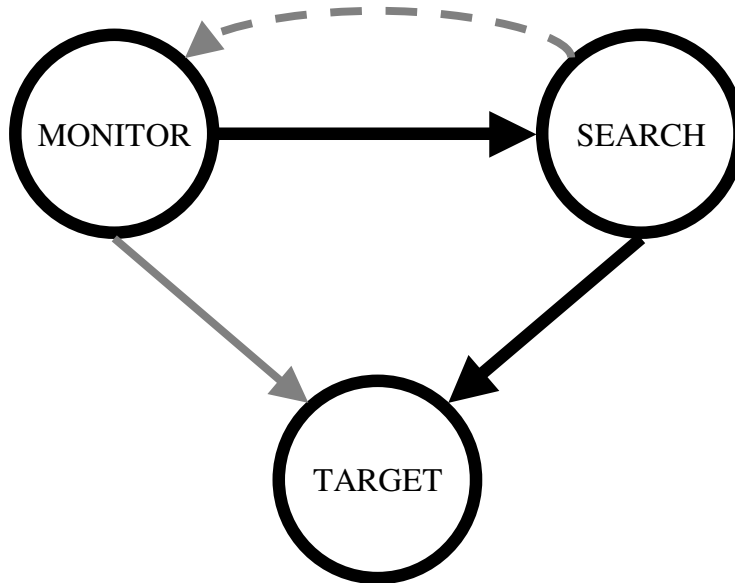


Figure 3: Control states for following the chemical gradient. Black arrows are the primary transitions near the target. The solid gray arrow is the possibility a robot bumps into the target before detecting the chemical, and the dashed gray curve is the reset transition.

necessarily optimal with respect to any particular performance measure. In particular, the choices of  $T_{\text{measure}}$  and  $C_{\text{threshold}}$  ensure the signal can be detected before the robot moves far downstream of the target, and also gives a fairly low false positive rate, as quantified in Section 7.

## 6.1 Brownian Motion

At low Reynolds number, passive motion of robots is primarily along the laminar streamlines of the fluid flow. Brownian motion gives an additional random component to the motion. The robots have only two states: MONITOR when waiting to bump into the target and TARGET when at the target. The concentration of MONITOR state robots  $R_m$  has the form of Eq. (3) but with diffusion coefficient for the robots rather than the chemical, which in steady-state is

$$\nabla \cdot (D_{\text{robot}} \nabla R_m - \mathbf{v} R_m) = 0 \quad (9)$$

## 6.2 Follow Gradient

Robots can find a chemical source by following the chemical concentration gradient. A key challenge for this control is during the time required to measure the gradient the robot continues to move with the fluid past the target. Fig. 3 shows the control states: MONITOR, SEARCH and TARGET, corresponding to the robot monitoring for high concentration, searching for the target and at the target, respectively.

In the SEARCH state, the robot continues to move with the fluid while estimating the gradient, so if it waits long enough to accumulate many counts, giving accurate gradient direction estimate, it will be far past the target. Instead, we consider estimates in a relatively short time  $T_{\text{measure}}$  while the robot is still near the target. If the measured difference in counts gives a signal-to-noise ratio estimate above a threshold  $\text{SN}_{\text{min}}$ , the robot moves with respect to the fluid in the direction of the higher count with speed  $v_0$ . Specifically, the robot considers several groupings of the sensors on its surface into two opposite halves. Let  $C_{\text{min}}$ ,  $C_{\text{max}}$  be the counts on the choice of halves giving the largest difference in counts. Using Eq. (8), the control decision is to move in the direction with the  $C_{\text{max}}$  counts provided

$$C_{\text{max}} - C_{\text{min}} > \text{SN}_{\text{min}} \sqrt{C_{\text{max}} + C_{\text{min}}} \quad (10)$$

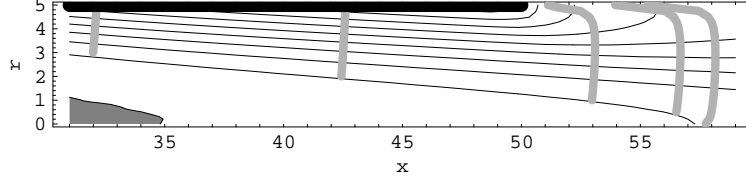


Figure 4: Concentration contours of signal chemical, and paths (in gray) following gradient for robots passing at several distances from the target, starting from the points where the signal-to-noise ratio reaches one. The figure shows a slice along the vessel, from the axis (at  $r = 0$ ) to the wall (at  $r = 5\mu\text{m}$ ). Distances along the axes are in microns. The dark gray region at lower left has concentration from target below that of the background. The section shown here is a small portion of the vessel cross section in Fig. 2.

Otherwise, the robot does not actively move, i.e., it continues to flow passively in the fluid.

Fig. 4 shows some ideal gradient-following paths through the chemical concentration near the target. Due to the axial symmetry of this scenario, the full 3-dimensional structure consists of rotations of the slice shown in the figure around the vessel axis. The concentration decreases much more rapidly radially, i.e., when moving from the wall toward the axis of the vessel, then when moving downstream at a constant distance from the wall. Thus the path following the gradient approximately first moves radially to the wall and then, if not at the target, moves upstream along the wall to the target.

Sensor noise leads to probabilistic gradient estimation, so this control technique performs a random walk with respect to the fluid biased in the direction of increasing concentration. To estimate the behavior of this random walk, the expected number of counts on the two opposite sides of the robot is  $(K_{\pm} + k)/2$  where the factor of 2 arises from considering counts to just one half of the robot, and  $K_{\pm}$  denotes Eq. (5) evaluated at a distance separation of  $a$  in the directions of increasing and decreasing gradient, respectively. These expected values and the Poisson distribution of actual counts determine the probability this control rule has the robot move in the correct direction (i.e., toward higher concentration), the wrong direction (i.e., toward lower concentration) or not move at all because the signal is too weak to distinguish from noise. Specifically, let  $P_{\pm}$  be the probability the criterion of Eq. (10) is satisfied in the directions of increasing and decreasing gradient, respectively. Then, on average, the robot velocity with respect to the fluid is  $v_0(P_+ - P_-)$  in the direction of the gradient and its diffusion coefficient is [5]

$$D_s = D_{\text{robot}} + \frac{1}{6}v_0^2 T_{\text{measure}} (P_+ + P_- - (P_+ - P_-)^2) \quad (11)$$

These values depend on the expected numbers of counts and hence on the control parameters  $T_{\text{measure}}$  and  $C_{\text{threshold}}$ . The net effect is for robots in the SEARCH state to have a larger diffusion coefficient  $D_s$  than that just due to Brownian motion, and an average velocity  $\mathbf{v}_s$  equal to the sum of its motion with respect to the fluid and the velocity of the fluid. Because these quantities are based on gradient measurements, they vary with robot position. When the signal is weak, Eq. (10) is unlikely to be satisfied, so  $P_+ \approx P_- \approx 0$  and the robot moves passively with the fluid. With a strong signal,  $P_+ \approx 1$ ,  $P_- \approx 0$  giving movement with respect to the fluid almost entirely in the direction of the gradient, with little additional diffusion. By contrast the robot paths in Fig. 4 ignore statistical errors in evaluating signal concentration gradient and Brownian motion

The concentration in steady-state near the target is governed by

$$\begin{aligned} \nabla \cdot (D_{\text{robot}} \nabla R_m - \mathbf{v} R_m) - \alpha_{m \rightarrow s} R_m &= 0 \\ \nabla \cdot (D_s \nabla R_s - \mathbf{v}_s R_s) + \alpha_{m \rightarrow s} R_m &= 0 \end{aligned} \quad (12)$$

The last term in these equations represents the transition from MONITOR to SEARCH when the chemical is detected. A robot in the MONITOR state detects the chemical and switches to the SEARCH state at a rate  $\alpha_{m \rightarrow s}$  given by Eq. (7). Similarly, the SEARCH state is characterized by  $D_s$  and  $\mathbf{v}_s$  values described above. In both states, the robots stick to the target if they bump into it, which is included as boundary conditions for these equations.

Eq. (12) does not include the much slower transition, shown as the dashed gray curve in Fig. 3, whereby a SEARCH state robot eventually returns to the MONITOR state if it no longer detects the chemical after a time

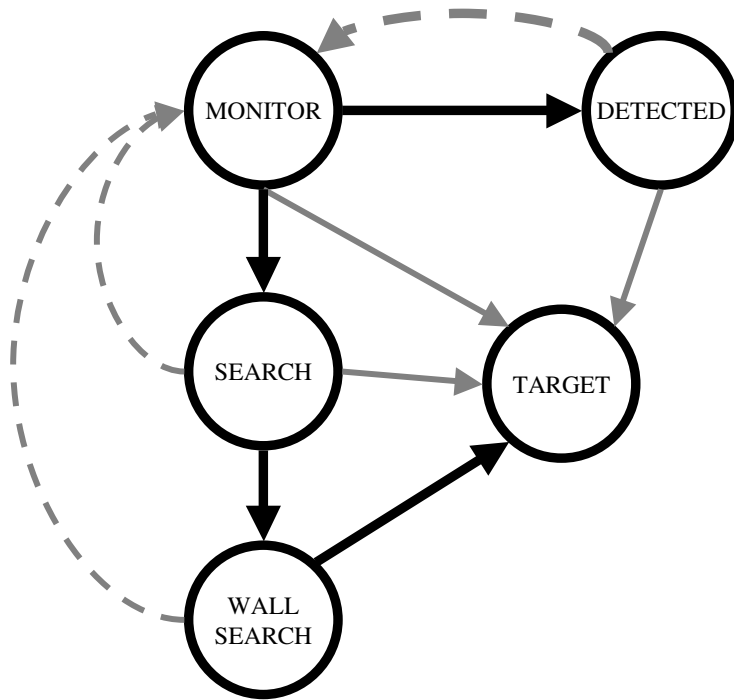


Figure 5: Control states for signaling detection of the chemical and having other robots respond. The transition types are indicated as in Fig. 3.

interval  $T_{\text{reset}}$ . This time interval is long enough to ensure the robot has moved well downstream of the target so the reset transition does not significantly affect the behavior of robots near the target. This transition also resets robots after a false positive detection.

### 6.3 Alert Other Robots to Chemical Signal

A difficulty with gradient following is the fluid motion during the time required to estimate the gradient direction, so robots typically must move upstream, against the fluid flow, to reach the target after detecting the signal. Another possibility is for robots detecting the signal to alert other robots still upstream of the target, using the control states given in Fig. 5. Then instead of the detecting robot attempting to reach the target itself, it can continue with the flow while those receiving the alert attempt to move to the vessel wall. This could allow some robots to reach the wall upstream of the target where they can then find the target via passive flow with the fluid.

Useful communication must reach robots upstream of the sender. In this control method, a robot detecting the chemical signal broadcasts its detection acoustically rather than using its energy to move to the target. Since typical distance between robots with parameters of Table 1 is  $\sim 60\mu\text{m}$ , a signal would need to be strong enough to be detectable, say,  $100\mu\text{m}$  from the source. This choice of signal distance is somewhat arbitrary. If chosen significantly smaller, often no following robot would be close enough to detect the signal. Conversely, a substantially longer signal range would likely be detected by multiple robots but have significantly larger power requirements (which grow quadratically with distance).

A robot in the MONITOR state waits for signals, chemical or acoustic. If it detects the chemical, it broadcasts a long range acoustic signal, changes to the DETECTED state and continues moving with the fluid. A MONITOR state robot receiving the acoustic signal switches to the SEARCH state. The robot then attempts to reach the vessel wall either through random motions in the fluid (significantly increasing its diffusion rate over that due to Brownian motion) or directed motion if its sensors enable determining the direction to the wall. We suppose the robot moves at a speed  $v_0$  with respect to the fluid. The robot continues until either it encounters the wall (changing to WALL SEARCH state) or for a time interval  $T_{\text{reset}}$  (and then returns to the



bump into it and manipulate their surface stickiness to allow them to move along the wall pushed by the fluid, e.g., by rolling. Specifically, robots receiving the signal could stick to the wall if they happen to bump into it, and then roll along the wall with the fluid flow until they either reach the target or the  $T_{\text{reset}}$  time limit. While such robots will not reach the target as often as those able to actively move, the communication could nevertheless improve on robots acting independently using Brownian motion to bump into the target.

The second strategy to reach the wall is similar to the first but uses robot locomotion ability to increase the effective diffusion rate. Specifically, the robots perform a random walk, by moving at speed  $v_0$  with respect to the fluid, with random changes in direction at a rate  $1/T_{\text{random}}$ . This random walk corresponds to a diffusion coefficient of  $D_s = v_0^2 T_{\text{random}}/3$  [5]. For the parameter choices of Table 2, this gives  $D_s = 300 \mu\text{m}^2/\text{s}$ , considerably larger than Brownian motion diffusion,  $D_{\text{robot}}$ . With this strategy for finding the wall, the robot continues moving with the fluid, so  $\mathbf{v}_s = \mathbf{v}$  in Eq. (13).

The third strategy assumes the robot can accurately determine the direction to the nearest part of the vessel wall, and it then moves in that direction with respect to the fluid. This case has no additional diffusion, so  $D_s = D_{\text{robot}}$  and  $\mathbf{v}_s$  equals  $\mathbf{v}$  plus  $v_0$  directed to the wall. Compared with random motions, directed motion allows the robot to reach the wall sooner, so it is less likely to be downstream of the target when reaching the wall. Hence directed motion increases the rate robots arrive at the target. In practice, sensors used to determine the direction to the wall will have some error, giving behavior intermediate between these two strategies of random and directed motions.

## 6.4 Alert and Guide Robots Toward Target

Acoustic signals can relay the detection of chemicals to robots still upstream of the target, alerting them to search for the target without needing to move upstream against the fluid flow. However, at the robot densities we consider, the acoustic signals must be fairly long range to have a reasonable likelihood of reaching even a single upstream robot. Depending on locomotion efficiency, the energy required for such acoustic signals can be comparable to that of the upstream motion when signals are not used.

Acoustic signal strength decreases as the square of the distance, so shorter-range signals is much more energy efficient. One approach to exploit this fact has some robots act as guides on the vessel wall. In this case, robots detecting the signal move to the wall as before but instead of then immediately searching for the target along the vessel wall, they temporarily attach to the wall and emit a sequence of short range acoustic signals, with just enough power to be detectable across the diameter of the vessel, e.g., about  $10 \mu\text{m}$ . While typically requiring about 10 repetitions before a signal is received by a single passing robot, each signal requires only  $1/100^{\text{th}}$  the energy of that of the long range signal. A few such guide robots on the wall a bit upstream of the target will likely be able to signal most of the passing MONITOR state robots.

At the extreme, only the first robot detecting the chemical would need to send an acoustic signal detectable over  $100 \mu\text{m}$  and then continue past the target, while the next robot, detecting the acoustic signal would move to the wall and anchor itself somewhat upstream of the target. This guide robot then signals all remaining robots. The corresponding control states shown in Fig. 7 allow for multiple guides, the possibility of some robots missing the signal from the guide and instead later detecting the chemical, and for guides to switch to the WALL SEARCH state to then go to the target.

Specifically, this control introduces one new state, GUIDE. Robots in the SEARCH state switch to the GUIDE state when first reaching the wall. While we could have SEARCH state robots reaching the wall in response to a guide signal immediately begin looking for the target, for simplicity in dealing with false positives we instead have all robots first become guides.

Guide robots emit a short range acoustic signal at a rate  $\omega$ . To avoid having robots remain as guides indefinitely in cases of false positive chemical detection, we have the guides change to the WALL SEARCH at a rate  $\alpha_{g \rightarrow w}$  specified as a control parameter. In the WALL SEARCH state, robots behave the same as in the previous control method which lacked guides.

The steady-state concentrations of robots in the MONITOR, DETECTED and SEARCH states,  $R_m$ ,  $R_d$ ,  $R_s$ , respectively, are governed by Eq. (13). The guide robots on the wall do not move, so their steady-state surface concentration on the wall  $R_g$  (i.e., number of robots per unit area) is just the balance between the flux of SEARCH robots reaching the wall,  $F_s$ , and the rate at which GUIDE robots switch to the WALL SEARCH state,  $\alpha_{g \rightarrow w}$ , giving  $R_g = F_s/\alpha_{g \rightarrow w}$ .

The MONITOR state robots change to the SEARCH state in response to an acoustic signal from either a

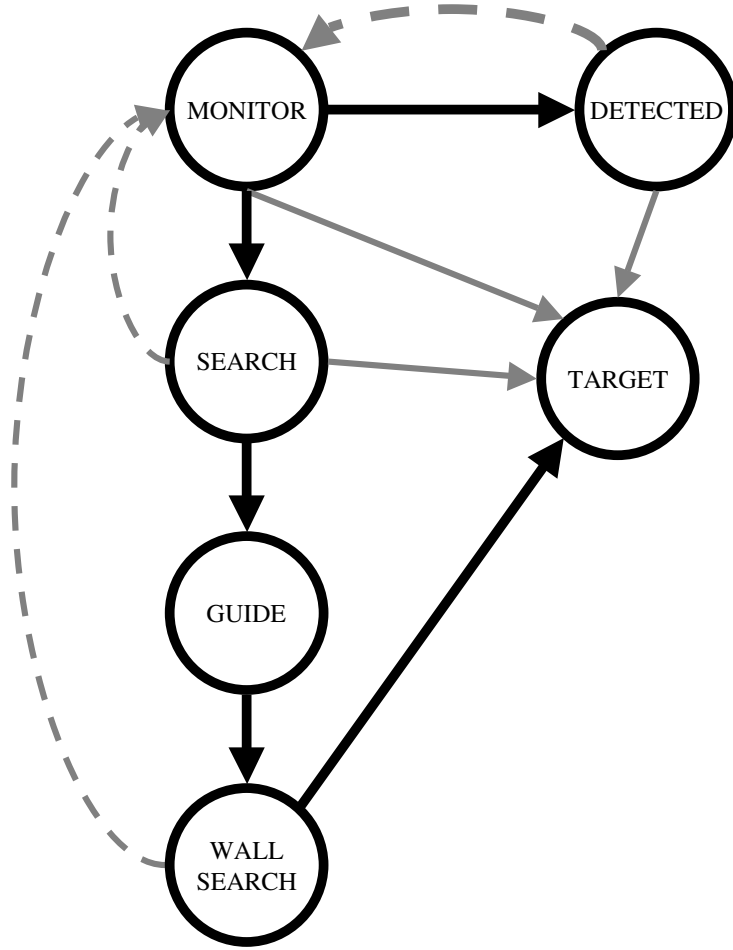


Figure 7: Control states for signaling detection of the chemical while other robots guide and respond to the target. The transition types are indicated as in Fig. 3.

robot detecting the chemical (as it switches to the DETECTED state) or from a guide robot. Thus  $\alpha_{m \rightarrow s}$  equals Eq. (14) plus an additional term for the average rate a MONITOR robot at a given location receives signals from the GUIDE robots within its detection range, i.e.,

$$\omega \int R_g dS \quad (15)$$

with the surface integral over the region on the wall from which the guide signals are detectable at the MONITOR state robot's location.

From the control perspective, the ratio  $\omega/\alpha_{g \rightarrow w}$  determines the average signal rate from guides. Increasing the signals by increasing  $\omega$  means each guide robot produces signals more rapidly, thereby increasing power use. Conversely, decreasing  $\alpha_{g \rightarrow w}$  increases the number of guide robots as each spends more time acting as a guide before searching for the target.

Although not included in the analysis of this method, a simple modification to the guide behavior could reduce power use further: when several guides are at the wall and close to each other, each will detect relatively strong signals from other guides. In this case they could reduce their signal range, the frequency with which they emit signals or increase their rate of switching out of the guide state to look for the target. The net effect distributes signals among multiple guides, thereby reducing power required to alert passing robots.

control method	target rate	output power use (fW)	
		acoustic	locomotion
Brownian motion	0.26	0	0
follow gradient	10.5	0	1.1
alert (random)	6.3	8.9	0.92
alert (directed)	6.8	8.9	0.19
alert (passive)	0.32	8.9	0
alert and guide (random)	12.8	3.9	1.8
alert and guide (directed)	13.1	3.9	0.38

Table 3: Rate robots reach the target (i.e., number of robots per second) and output power use (in femtowatts, i.e.,  $10^{-15}\text{W}$ ) in steady-state. For control methods involving robots moving to the vessel wall, values are given for both random and directed motions to the wall.

## 7 Robot Performance

The previous section described four control methods: passive search for the target via Brownian motion, individually detecting and following the chemical signal to the target, and two approaches to coordinating behavior with acoustic signals. Numerically solving the diffusion equations for the concentrations of robots in the various control states gives the steady-state behaviors. In particular, the total flux to the target gives the average rate at which robots arrive at the target. For power use due to locomotion, a robot moving with respect to the fluid with speed  $v_0$  dissipates  $6\pi a\eta v_0^2$  from Eq. (2). Thus the average power use for locomotion within the vessel is the volume integral of this quantity times the concentration of moving robots, i.e.,  $R_s$ , since that is the only state in which robots actively move in the vessel.

Table 3 summarizes the behaviors for these control methods using the control parameters of Table 2. The total flux of robots entering the vessel, and hence the maximum possible rate at which robots could reach the target, is 15.7 robot/s. A variety of control approaches allow robots to find the target, in spite of its small size and the limited time available to detect the chemical before the fluid flow moves a robot far downstream of the target.

Robots without locomotion capability can detect the chemical from the target, but only a few actually reach the target via Brownian motion. The “alert (passive)” entry shows the modest improvement communication gives over just using Brownian motion to bump into the target. The behavior of “alert and guide” for such robots is essentially the same: so few robots reach the wall by Brownian motion that guides are too infrequent to improve performance.

Active control with locomotion enables more rapid response to the target. One approach follows concentration gradients in addition to just detecting the high concentration. In this case, the chemical concentration is sufficient to allow most passing robots to detect the chemical with the parameters of Table 2, but about a third of the robots are unable to reliably estimate the gradient, according to the criterion of Eq. (10), before moving far downstream from the target. Another approach avoids the challenge of significant motion upstream against the fluid flow by communicating chemical detection to upstream robots. Adding the GUIDE state reduces the required communication energy.

The acoustic power values use a nominal energy of  $E_{\text{signal}} = 10^{-15}\text{J}$  for a single long-range acoustic signal, and 100 times less for a short-range signal. The table lists output power for the operations. Input power levels required to deliver these outputs are obtained from these values by dividing by the power efficiencies of acoustic signal generation and locomotion,  $\epsilon_a$  and  $\epsilon_{\text{loc}}$ , respectively.

For controls using directed motion to the wall, the values in Table 3 include neither power for sensors determining the direction to the wall nor effects of sensor noise. Thus the behavior for directed motion to the wall represents a best case evaluation.

### 7.1 Control Trade-Offs

To visualize the results in Table 3, Fig. 8 compares the energy used to deliver one robot to the target as a function of locomotion efficiency,  $\epsilon_{\text{loc}}$ . This energy use includes both the activities of the robot reaching

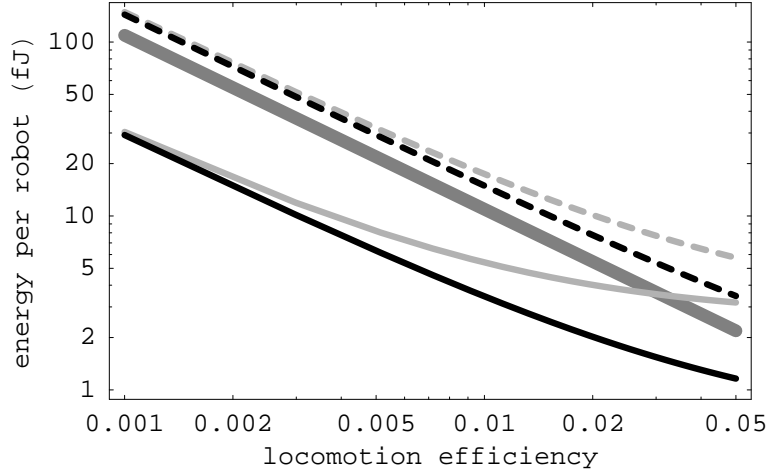


Figure 8: Energy use, measured in femtojoules (fJ), per robot reaching the target for various control methods. The thick, dark gray curve is for gradient following. The black and light gray sets of curves are for acoustic signals, with and without the guides, respectively. Within each set, the dashed curve is for random motion to find the vessel wall and the solid curve is for directed motion.

the target as well as a proportionate share of activities of other robots (e.g., for acoustic signaling) that help guide it to the target. The figure uses values of Table 3 with acoustic efficiency of  $\epsilon_a = 0.5$ , a plausible value for operation at the ultrasound frequencies we considered [23]. For comparison, Brownian motion uses no energy per robot reaching the target, but also gives a low response rate. The energy use discussed here does not include energy for internal operations of the robot, e.g., for its computer or sensors.

At low locomotion efficiencies, control methods using communication can perform better than gradient following. Separating the roles of detecting the chemical and moving to the target deals with the difficulty inherent in diffusing chemicals in flowing fluids: high concentrations are somewhat downstream of the target where response involves moving upstream. Provided the robots detecting the signal can communicate with those upstream for modest cost and robots can estimate direction to the wall, this division of roles is beneficial. Using guides with short range communication improves performance further. In terms of device fabrication, this illustrates a potential design trade-off between improving mechanical locomotion efficiency or adding communication capability.

## 7.2 False Positives

In addition to finding the target, control design should also handle false positives, i.e., robots incorrectly deducing a target is nearby due to statistical fluctuations from the background chemical concentration. In our case,  $\alpha \approx 7.6$  molecule/s reach a robot from the background concentration, giving a probability  $P_{\text{false}} = 2.7 \times 10^{-3}$  to have two or more counts in a 10ms interval. This false positive probability, associated with the choices of Table 2, is small for any single measurement interval. However, there are many more opportunities for false positives than the single true positive at the target. For instance, if the devices are activated via an external signal in a centimeter-sized volume and take time  $t$  to move through the volume, each robot will have about  $t/T_{\text{measure}}$  opportunities for detecting a signal with no target as it passes through the volume, and hence  $N_{\text{false}} = P_{\text{false}}t/T_{\text{measure}}$  false positive detections, on average.

For an upper bound on number of false positives, assume flow through the entire volume is the same slow speed as in the tiny vessel with the target. Then  $t$  is about 10 seconds, giving  $N_{\text{false}} = 2.7$  false positives, on average. The control algorithms must not have robots stop their motion indefinitely (e.g., by sticking to the vessel wall until they receive enough counts to estimate the concentration gradient) when they detect a signal. Otherwise, the false positives would prevent robots from ever reaching the target. We avoid this difficulty in the control algorithms presented in this paper by having the robot transition back to the monitoring state if it is unable to find the target after a time interval  $T_{\text{reset}}$ .

control method	target rate	output power use (fW)	
		acoustic	locomotion
Brownian motion	0.17	0	0
follow gradient	10.8	0	2.7
alert (random)	2.0	8.9	0.91
alert (directed)	2.3	8.9	0.19

Table 4: Rate robots reach the target (robot/s) and output power use (in femtowatts, i.e.,  $10^{-15}\text{W}$ ) for target oriented lengthwise along the vessel.

The false positive detections require additional energy use, beyond that of Table 3 used by robots passing the target. This extra energy is significant for robots using a fixed fuel source. For such robots, minimizing power use would be a major concern and the false positive rate could be lowered (e.g., by increasing  $C_{\text{threshold}}$  in Table 2) at the expense of reducing the number of robots finding the target.

The false positive rate determines the behavior of robots that do not pass the target, which will be most robots for scenario considered in this paper. The entire response of such robots will be false positive detections. A safety issue is the power dissipation from these robots. Consider the upper bound of transit time  $t$  around 10 seconds giving  $N_{\text{false}} = 2.7$  detections per robot. In the control algorithms presented here, the robots actively move only a portion of the time (e.g., when they have a significant gradient signal). But as an upper bound on power use, suppose after each detection the robot moves at speed  $v_0$  through the fluid for the full reset time  $T_{\text{reset}} \approx 100\text{ms}$ . In that case, at any given time about  $N_{\text{false}}T_{\text{reset}}/t = P_{\text{false}}T_{\text{reset}}/T_{\text{measure}} \approx 0.03$  of the robots would be in motion. As a rough estimate on total power dissipation, such a tissue volume would have about  $0.1\text{cm}^3$  of blood volume and hence about  $4 \times 10^6$  active robots, dissipating a total of about one microwatt. This upper bound on robot power use is orders of magnitude below resting metabolic power use. Even with the low value of  $P_{\text{false}}$ , the vast majority of robots detecting the chemical will in fact be responding to false positives.

The false positive response is also relevant for other safety issues. In particular, significant robot motions throughout the volume of tissue could damage vessel walls from collisions. Collisions are mainly an issue with the control using random motion to find the wall. Other control methods discussed in this paper are less likely to involve collisions with the wall. For instance, in the case of false positives, the gradient following control method will have most robots moving passively with the fluid since they will not detect enough difference in counts between sides to activate the gradient following motion. Furthermore, if robots have the sensing ability to detect the wall, they could slow down as they approach the wall. At any rate, the robot speed  $v_0$  in Table 2 is likely below the speed at which collisions with the vessel walls cause damage [24]. Nevertheless, as with other safety issues of microscopic robots, experimental evaluation will be necessary and the control choices for the robots should minimize the potential for injury while successfully performing their tasks.

## 8 Alternate Task Geometries

The target geometry considered above, shown in Fig. 1, is only one possible arrangement for the target in the vessel wall. To examine the robustness of the control approaches, this section describes results for additional situations.

The controls described above using communication involve passive motion once a robot reaches the wall. Such robots will find the target only if they reach the wall at or upstream of the target. These responding robots move toward the wall before encountering detectable chemical concentrations. Thus the robots lack a guide to the best locations on the wall. With the axially symmetric geometry of Fig. 1, such guidance is not needed: any point on the wall upstream of the target moves passively to the target. However, if the target does not wrap around the vessel some upstream locations will not lead to the target. To examine the behavior in this case, we consider a target with the same surface area as in Fig. 1 but oriented lengthwise along the vessel. A specific example is a target extending only  $1/3$  of the way around the vessel and with three times the length, i.e.,  $90\mu\text{m}$ , along the vessel. In this case, the chemical spreads around the vessel as it moves

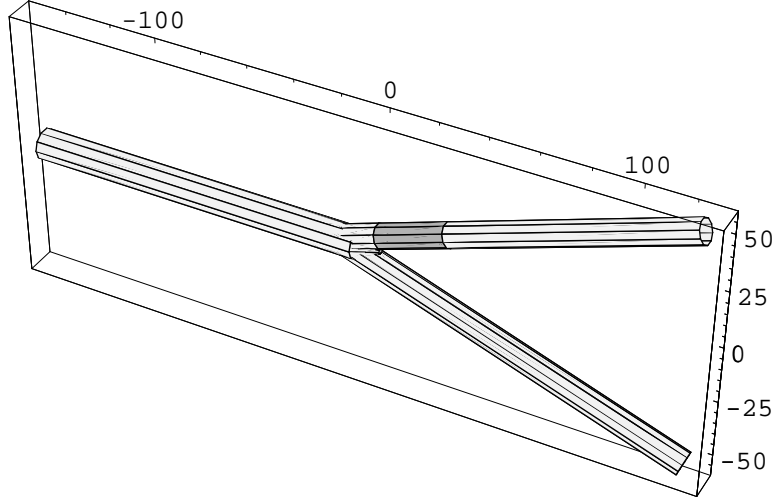


Figure 9: Chemical source (gray area) located near a vessel branch. Distances are in microns.

downstream.

Table 4 shows the resulting behaviors. For Brownian motion alone, the robots find the target only about 65% as often as for the equivalent area target wrapped around the vessel. Given the fairly small displacements during the time the robot passes the target, this reduction can be understood as due to only  $1/3$  the vessel wall having the target, but the target being 3 times longer so robots spend 3 times as long passing it, increasing the Brownian displacement by a factor of  $\sqrt{3}$ . Combining these effects suggests the effectiveness of Brownian motion should decrease by about  $\sqrt{3}/3 = 0.58$ , close to the observed ratio.

Following the concentration gradient gives about the same flux of robots to the target as when the target wraps around the vessel. The robots have somewhat larger power use due to the longer distance to the target and weaker gradient signal for robots passing near the wall opposite the target location. Quantitatively, the average distance from a robot moving with the fluid to the target on the vessel wall is about 1.8 times as large for this lengthwise target geometry, compared to an increased power use of a factor of about 2.5, so the change in direct distance to the target accounts for only part of difference in power use.

The controls using acoustic signals give about  $1/3$  the number of robots reaching the target. This is understandable since these communication controls have robots move passive once they reach. Since the target only extends around  $1/3$  of the vessel wall, it captures only this fraction of the robots. In this case, using acoustic signals to avoid measuring gradients is effective in allowing robots to respond before they pass the target, but does not enable robots to locate the target's position around the vessel wall. This issue also arises in the control using guides to reduce acoustic signal power.

The behaviors discussed above, as well as simulations in previous studies [13], consider a target on the wall of a long pipe of uniform thickness. Targets near a branch of the circulation raise further issues because the branches restrict the volume through which the chemical can move and alter the fluid flow from the parabolic form of Eq. (1).

As a specific example, Fig. 9 shows the geometry of two vessels of radius  $R = 5\mu\text{m}$  of Table 1 connecting to a slightly larger vessel. For the circulatory system, flow is generally faster in larger vessels, implying the total cross section of the smaller branches exceeds that of the larger vessel. Quantitatively, branching vessels roughly conserve the sum of the cubes of their diameters [57]. For a split into two branches of equal diameters shown in Fig. 9, the corresponding radius of the larger vessel is  $\sqrt[3]{2} R$ , with modestly faster fluid flow. In the figure, the branches have angles  $\pm 20^\circ$  with respect to the larger vessel. The target area is the same length as in Fig. 1 and wraps around the upper vessel.

The gradient following and communication controls respond differently depending on the direction of flow. When the flow is from the smaller vessels into the larger one (“merging”) the communication protocols have little effect on the number of robots reaching the target: those protocols rely on robots moving to the wall

upstream of the target and then moving passively until they reach the target. Since the branch is downstream of the target in this case, robots entering the larger vessel are already downstream of the target and their response to the acoustic signals leads them to the wall of the larger vessel and hence away from the target. Such robots could respond to the chemical concentration gradient. However, the laminar fluid flow at low Reynolds number gives little mixing of fluid from the merging vessels. This means the chemical from the target doesn't significantly reach the far side of the larger vessel until it has moved significantly downstream from the branch. To quantify this, the fluid takes time  $\approx d/v_{\text{avg}}$  to move a distance  $d$  downstream from the branch, during which the chemical will diffuse a distance  $\sqrt{6Dd/v_{\text{avg}}}$ . This reaches the far side of the vessel only after about  $100\mu\text{m}$  or so from the branch, at which point the concentration is fairly low. Thus we can expect robots from the lower branch will be far downstream from the target before detecting the chemical, at which point the concentration will be too low for effective gradient estimation. Thus we can expect most robots from the lower branch will not find the target. Numerical solution to Eq. (12) with this branch geometry confirms this expectation: robots reach the target at the rate 10.8robot/s, only slightly higher than the result in Table 3. They use more power, about 5fW due to some of the robots from the lower branch detecting the chemical and then attempting to find the target, mostly unsuccessfully.

Flow in the other direction, from the larger to smaller vessels ("branching"), does not change gradient following control: in this case, robots detect the signal at or downstream of the target. Those robots in the larger vessel or in the other branch will not detect the chemical signal. With the acoustic signals, robots approaching the branch in the larger vessel will respond by moving to the walls. However, with no further guide as to which part of the wall leads to the branch with the target, this behavior does not increase the number of robots moving into the branch with the target and hence does not change the rate robots find the target.

From this discussion we see alternate target shape and vessel branching alter the quantitative performance of the robots but not by a large factor. Thus the simple control methods of this paper are fairly robust with respect to changes in the geometry. Thus studies based on the simple scenario of a flow in a single uniform vessel can also capture order-of-magnitude performance estimates for a wider range of scenarios.

While some applications of microscopic robots could involve finding chemical sources in largely empty fluid, the most significant potential uses in vivo would involve fluids containing a significant fraction of objects, such as cells. The schematic in Fig. 10 illustrates this situation for a robot in a small blood vessel. The cells, most of which are red blood cells, occupy about 1/5-th of the volume, a typical *hematocrit* value for small blood vessels. Thus the vessel is quite crowded, with continually changing geometry as cells move, rotate and distort with the fluid. The moving cells significantly affect the distribution of diffusing chemical signals and the motion of the robots.

A simple model of the effect of cells [38] is an increase the effective diffusion rate of the chemicals and robots to about  $1000\mu\text{m}^2/\text{s}$  for the fluid speeds and vessel sizes we consider. At this large a diffusion coefficient for the robots, all the control methods deliver about 14 robots per second to the target, out of a total of 15.7robot/s passing through the vessel. However, the increase in diffusion is unlikely to be this large for behaviors near the vessel walls [38], which are most important for robots reaching the target through random motion alone. Moreover, while this approximation of the effect of cells in the fluid is reasonable for the chemicals, the robots' size is comparable to that of the vessel and cells so hydrodynamic effects are likely to be more significant than an increase in random motions. The effect of cells also depends on the size of the vessels. In particular, the smallest vessels are about the same size as cells so the cells go through one at a time, with less freedom for rotation to mix the chemical. Evaluating behavior in these cases will require more extensive modelling of the interaction among the cells, robots and the fluid flow.

The brief discussion of alternate geometries in this section suggests additional control strategies. For instance, to better handle various target shapes and exploit the possibility of other nearby vessel branches, the WALL SEARCH robots used in the communication protocols could also monitor for chemical signal and actively follow the concentration gradient along the wall if they can detect it. This would be especially useful when the target does not extend most of the way around the vessel. Furthermore, guides could not only alert passing robots but could also indicate where the robots should go. For example, robots could emit a short-range signal when they first detect a guide's alert signal, causing nearby guides to emit more frequent signals and allowing the passing robot to move toward higher signal strength (either directly, if it can determine the direction, or via a biased random walk by comparing how strength changes with time). Such guide signals could both to guide robots to the correct part of the vessel wall and to the correct branch in branching vessels.

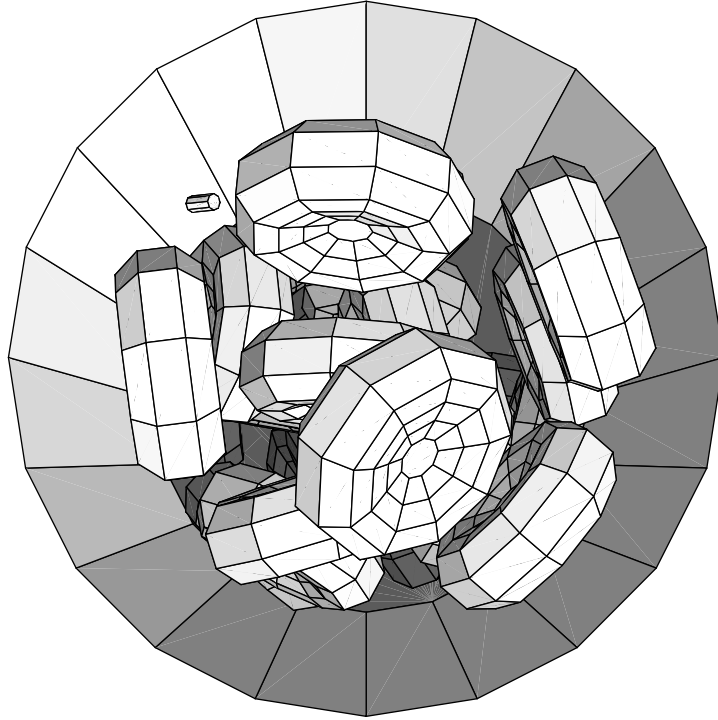


Figure 10: Internal schematic view of a 20-micron diameter vessel showing cells and one robot (represented as a small cylinder near the wall at the upper left). The robot is considerably smaller than the  $\sim 7\mu\text{m}$  cell diameter.

More generally, the behavior of controls aggregating robots to targets depends on *local* concentration of the robots, e.g., doubling the local density of robots doubles the response rate. Hence additional cooperative control could act to locally increase the concentration. As an example of cooperating to improve performance, in a more realistic situation with multiple branching vessels, relaying acoustic messages sufficiently far upstream to reach branch points, and then having guide robots remain at those points, could be used to alter the distribution of robots in the vessels, e.g., to attract more robots to vessels where targets have been found. Such a collection of guide robots would form a temporary messaging network to locally increase concentrations of responding robots.

## 9 Discussion

This paper described how the physics of microscopic robots operating in fluids affects choice of control method. Several simple swarm controls can reliably find chemically distinctive targets as small as a single cell, and also handle false positive detections. Thus various hardware configurations can give adequate performance, e.g., with or without long range communication. The results show how control choices can compensate for limited hardware (e.g., sensor errors or power limitations), providing some hardware design freedom. Thus theoretical studies incorporating the main physical properties of the environment and robots, such as presented in this paper, help determine alternate hardware performance capabilities needed to provide robust systems-level behavior.

The results presented here establish feasibility of simple controls, but are not likely to be optimal for any particular task either in terms of performance or hardware requirements. Identifying the best choices for control parameters, such as those in Table 2, would extend this work on *feasibility* to *optimal* coordinated control techniques. Formalisms for optimizing multiagent systems design have been developed in the

context of larger robots. One such approach is the stochastic analysis technique used in this paper, which has been experimentally compared to behavior of larger robots [40]. Another formalism treats agent action and communication under uncertainty as a decision theoretic problem, selecting among individual action and communication with others when both have costs and uncertain benefits. Specifically, the randomness from Brownian motion and sensor noise along with limited robot capabilities make the partially-observable Markov decision problem formalism [12] well-suited for describing microscopic robot tasks. The behaviors discussed in this paper can provide key ingredients for this formalism, e.g., the probability distributions for encountering detectable concentrations and of distances between robots to determine required communication power. In principle, these values allow determining optimal control actions. Finding such controls can be computationally intractable, but heuristic methods give reasonable choices in at least some cases involving limited communication choices and few agents [49, 30]. Evaluating such heuristics for the physical environments of microscopic robots is an interesting direction for extending this work. Furthermore, evolutionary techniques for swarm coordination [19] are also of interest as they may identify new strategies not easily found otherwise due to the unfamiliarity of physics of microscopic environments. Such strategies may be especially helpful for robots changing from widely separated independent actions to detailed coordination as they aggregate at small target areas.

As a caveat on the applicability of the results for behavior in blood vessels, the task examined here treats the vessel walls and all objects as rigid geometric shapes. We do not consider changes in the overall fluid flow (e.g., in response to injury or temperature) or deformations of the vessel walls, which require more complex models [9]. The task environment examined here does not include cells in the fluid, nor dynamical responses of the cells forming the vessel wall (e.g., creating gaps to allow some immune cells to leave the vessel).

A more complete analysis of the task scenario would include additional physical effects. For instance, specifying a particular locomotion technique (e.g., flagella) and including hydrodynamic effects on the robot motion would improve estimates of the robot power requirements. Hydrodynamic effects become especially significant when the distance between robots is only a few times their size [51], as would occur when robots aggregate.

Due to the approximations used in this paper, the results will not quantitatively agree with actual behaviors in blood vessels. This issue also arises for studies of larger robots [10], where quantitative agreement between simulations and actual behavior requires extensive empirical evaluation [35]. Such evaluation, including studies of the microscopic dynamical properties of cells and vessel walls (for which nanorobots would be useful research tools), will be required for more accurate nanorobot behavior studies. Nevertheless, the results reported in this paper should give order of magnitude estimates of behaviors and establish the feasibility of the tasks for plausible physical behaviors and robot capabilities. In spite of these complications, the simple task treated in this paper indicates the importance of considering the discrete molecular nature of chemical sensing and physics of viscous flow. It also provides behaviors in a simple task environment to help validate more complex simulations. In particular, the results indicate various design constraints on the robots. For instance, the concentrations of chemicals released in response to injury are low enough that a robot only encounters a few molecules while in the vicinity of the target area, so statistical fluctuations in the number encountered are a major source of sensor noise, no matter how sensitive the sensor itself is. Typical fluid flow speeds and chemical diffusion coefficients prevent the chemical from moving much upstream of the target, so robots depending on chemical signals alone won't detect the signal until they are at or even past the target location.

The behaviors examined in this paper also indicate how the simple control strategies will perform poorly with even more exacting physical requirements. In particular, if the chemical of interest had a concentration near the target about 10 times smaller than that of Table 1, it would be difficult to detect before passing well downstream of the target with any choice of measurement time and threshold, without also introducing a high false positive rate. Such scenarios would need a more elaborate control strategy. For example, robots could occasionally move to the wall and spend more time measuring concentration while stuck to the wall to gain more accurate concentration estimates. Alternatively, communication could substitute for the weak concentrations: the occasional robot finding the target through Brownian motion could emit signals to alert passing robots, most of which would otherwise pass the target without detecting the low concentration chemical. A similar difficulty would arise if the target area were considerably smaller than considered here.

Beyond the specific results on control performance, the approach to evaluating robot behaviors used here [27] allows evaluating average physical behaviors of microscopic robots in a variety of task scenarios.

This approach is not limited to the steady-state behaviors examined here: the diffusion equations can also address time-dependent scenarios by including the time-derivative term of Eq. (3). A significant limitation of this approach arises from the difficulty in modeling more elaborate controls involving conditional behaviors based on many events in individual robot histories. In such cases, the robot behavior is not determined primarily by its local environment, but also by the environment encountered in its past. To some extent, such controls can be addressed with additional variables, such as the integrated counts during the motion through the fluid of Eq. (5). Or a finer-grained model of the robot state (e.g., distinguishing robots with differing numbers of previously encountered molecules) could be used. Taking this to the extreme, each robot would be considered individually based on its unique history, leading to an agent-based simulation instead of the aggregate average treatment used here. Nevertheless, even in these cases the aggregated diffusion equations can still give a rough guide to average behaviors, allowing selection of promising control parameters for more detailed simulation studies. Conversely, control methods involving robot histories could be modified to allow more accurate aggregate modeling. For example, controls specifying an action taken after a set time interval  $T$  introduce a historical dependence in the robot controllers. If instead the action is initiated stochastically at a fixed *rate* so the *average* time interval until the action is  $T$ , then the control no longer depends on robot history. Although these two controllers have slightly different behavior, they are similar on average. Moreover, errors in robot control decisions (e.g., due to sensor noise) will also introduce a stochastic element into even nominally fixed control choices, reducing the difference between these approaches in practice.

We considered homogeneous robots, i.e., all with the same control program and capabilities. More generally, robots could have different capabilities, e.g., some to act as scouts with a wide range of sensors, others to provide additional power, and others with large supplies of specific chemicals useful for treating an injury once it is located. Initially homogeneous robots could also develop temporary or permanent differences based on their history, e.g., the level of their energy reserves influencing whether they switch to roles demanding high or low power. Such heterogeneous teams face additional control issues of resource allocation, for which market-based control [15] should be well-suited due to the large numbers of robots and limited effect of any one robot. Heterogeneity involving robots of different sizes can also be useful when the task requires coordinated behaviors on several biological scales from individual cells to tissues [56, 32].

More elaborate controls could communicate not just an alert signal but also the strength of the detected chemical (i.e., number of sensor counts), and length of time over which high signal detected. For controls using guides, robots reaching the target could emit a signal to the guides indicating the target was actually found, and the guides subsequently communicating this increased reliability of detection to passing robots. Robots receiving this additional reliability information could adjust their response. For instance, more reliable signals could lead robots to search longer before they abandon their search. While such additional communication can improve performance, it is also important to be careful of errors in such “definite target” signals so single mistakes are not amplified throughout the population of robots. Hence it remains useful to have probabilistic control rules switching robots back to their default monitoring state rather than, say, a single robot signal switching other robots into search mode until they find a target, which could continue indefinitely when in fact there is no nearby target. Identifying robust communication protocols for computationally-limited agents is a useful direction for further research, not only for microscopic robots but also for larger swarm behaviors relying on single signals to affect behaviors of many robots as in some proposals for modular robotics [7, 52].

Another use for short-range communication, if robots can determine the approximate direction of the signal, is to improve gradient estimation. In particular, from Eq. (5) and Eq. (8) the signal to noise ratio for gradient estimates grows as the three-halves power of the distance over which concentration is compared. Thus robots separated by  $5\mu\text{m}$  could share their concentration measurements to estimate gradients about 10 times faster than a robot by itself.

Beyond just finding a target, it would be interesting to examine subsequent activities at the target. One example is arranging for an appropriate number of responding robots. By monitoring the concentration of a short-range chemical or acoustic signal from others, a robot can estimate the number of robots at the target, in analogy with quorum sensing in bacteria [43]. The robot could use this information to determine when enough robots are at the target, thereby either leaving the target region itself or signalling to other passing robots to ignore the chemical signal from the target. Once robots aggregate to a given area, local controls developed for larger modular robots based on artificial “scents” passed among neighbors can form a variety of structures [7, 52] either static or dynamically responding to changing forces in the environment. These techniques readily apply to nanorobots since they do not require a centralized planner with extensive

computational capabilities or global knowledge of the environment. Hydrodynamic effects could also be useful for short range sensing or communication among robots, and quite different from experience with larger robots.

Another interesting task for chemical sensing microscopic robots is finding a chemical source moving either passively in the fluid or actively. Examples include pathogens in the bloodstream releasing a distinctive chemical. Further extensions include expanding the task beyond a segment of one vessel to investigate larger-scale navigation issues and multiple signal sources (e.g., a single injury site in the tissue giving rise to signals in many nearby blood vessels). A more complete analysis of response to injury would also include time-dependent signals and immune system response developed over the seconds to days following the injury or infection.

Safety is an important design criterion for medical applications. Thus, control programs should allow for sensor errors, failures of individual robots or variations in environmental parameters. For the simple distributed controls discussed in this paper, the statistical aggregation of many robots' choices provides some robustness against these variations, a technique recently illustrated using DNA computing to respond to patterns of chemicals [4]. In the context of multiagent control, signals from the environment or other robots should be treated as heuristics, i.e., suggestions requiring further confirmation, so that a single incorrect signal from a robot does not cascade into inappropriate actions by many other robots. More generally this leads to security issues surrounding the communication among nanorobots [33], and also arises in scent-based control programs used in modular robotics [7, 52]. Furthermore, the devices must be compatible with their biological environment, for at least enough time to complete their task. Appropriately engineered surface coatings and structures [24] should prevent unwanted inflammation or immune system reactions during their operation.

Even before their use with active controls, nanorobots acting as passive sensors could study the microenvironments in the body, by collecting information on small space and time scales. Such nanorobots will be useful not only as diagnostic tools and sophisticated extensions to drug delivery capabilities [2], but also as an aid to develop robot designs and control methods for more active tasks.

Studies of multiagent control behaviors for the unique physical properties of microscopic robots help identify their suitability for various tasks and provide design guidelines for various applications, e.g., the required number of robots, sensor accuracy, locomotion speed and power consumption. Multiagent systems, which focus on distributed, autonomous behaviors, give a useful design framework for coordinating large numbers of microscopic robots in a variety of task environments.

## Acknowledgments

I thank A. Casal, A. Cavalcanti, L. Rosen and J. Shi for helpful comments.

## References

- [1] J. P. Adler. Chemotaxis in bacteria. *Science*, 153:708–716, 1966.
- [2] Thresa M. Allen and Pieter R. Cullis. Drug delivery systems: Entering the mainstream. *Science*, 303:1818–1822, 2004.
- [3] Daniel Arbuckle and Aristides A. G. Requicha. Active self-assembly. In *Proc. of the IEEE Intl. Conf. on Robotics and Automation*, pages 896–901, 2004.
- [4] Yaakov Benenson, Binyamin Gil, Uri Ben-Dor, Rivka Adar, and Ehud Shapiro. An autonomous molecular computer for logical control of gene expression. *Nature*, 429:423–429, 2004.
- [5] Howard C. Berg. *Random Walks in Biology*. Princeton Univ. Press, 2nd edition, 1993.
- [6] Howard C. Berg and Edward M. Purcell. Physics of chemoreception. *Biophysical Journal*, 20:193–219, 1977.
- [7] Hristo Bojinov, Arancha Casal, and Tad Hogg. Multiagent control of modular self-reconfigurable robots. *Artificial Intelligence*, 142:99–120, 2002. Available as arxiv.org preprint cs.RO/0006030.
- [8] Eric Bonabeau, Marco Dorigo, and Guy Theraulaz. *Swarm Intelligence: From Natural to Artificial Systems*. Oxford University Press, Oxford, 1999.

- [9] Krzysztof Boryczko, Witold Dzwinel, and David A. Yuen. Dynamical clustering of red blood cells in capillary vessels. *J. of Molecular Modeling*, 9:16–33, 2003.
- [10] Rodney A. Brooks. Artificial life and real robots. In F. J. Varela and P. Bourguine, editors, *Proc. of the First European Conf. on Artificial Life*, pages 3–10, Cambridge, MA, 1992. MIT Press.
- [11] Arancha Casal, Tad Hogg, and Adriano Cavalcanti. Nanorobots as cellular assistants in inflammatory responses. In J. Shapiro, editor, *Proc. of the 2003 Stanford Biomedical Computation Symposium (BCATS2003)*, page 62, Oct. 2003. Available at <http://bcats.stanford.edu>.
- [12] Anthony R. Cassandra, Leslie Pack Kaelbling, and Michael L. Littman. Acting optimally in partially observable stochastic domains. In *Proc. of the 12th Natl. Conf. on Artificial Intelligence (AAAI94)*, pages 1023–1028, Menlo Park, CA, 1994. AAAI Press.
- [13] Adriano Cavalcanti. Assembly automation with evolutionary nanorobots and sensor-based control applied to nanomedicine. *IEEE Trans. on Nanotechnology*, 2:82–87, 2003.
- [14] Adriano Cavalcanti and Robert A. Freitas Jr. Autonomous multi-robot sensor-based cooperation for nanomedicine. *Intl. J. of Nonlinear Sciences and Numerical Simulation*, 3:743–746, 2002.
- [15] Scott H. Clearwater, editor. *Market-Based Control: A Paradigm for Distributed Resource Allocation*. World Scientific, Singapore, 1996.
- [16] C. P. Collier et al. Electronically configurable molecular-based logic gates. *Science*, 285:391–394, 1999.
- [17] H. G. Craighead. Nanoelectromechanical systems. *Science*, 290:1532–1535, 2000.
- [18] Amit Dhariwal, Gaurav S. Sukhatme, and Aristides A. G. Requicha. Bacterium-inspired robots for environmental monitoring. In *Proc. of the IEEE Intl. Conf. on Robotics and Automation*, 2004.
- [19] Marco Dorigo. Swarm-bot: An experiment in swarm robotics. In P. Arabshahi and A. Martinoli, editors, *Proc. of the IEEE Swarm Intelligence Symposium (SIS2005)*, pages 192–200, 2005.
- [20] K. Eric Drexler. *Nanosystems: Molecular Machinery, Manufacturing, and Computation*. John Wiley, NY, 1992.
- [21] David B. Dusenbery. Minimum size limit for useful locomotion by free-swimming microbes. *Proc. Natl. Acad. Sci. USA*, 94:10949–10954, 1997.
- [22] David B. Dusenbery. Spatial sensing of stimulus gradients can be superior to temporal sensing for free-swimming bacteria. *Biophysical Journal*, 74:2272–2277, 1998.
- [23] Robert A. Freitas Jr. *Nanomedicine*, volume I: Basic Capabilities. Landes Bioscience, Georgetown, TX, 1999. Available at [www.nanomedicine.com/NMI.htm](http://www.nanomedicine.com/NMI.htm).
- [24] Robert A. Freitas Jr. *Nanomedicine*, volume IIA: Biocompatibility. Landes Bioscience, Georgetown, TX, 2003. Available at [www.nanomedicine.com/NMIIA.htm](http://www.nanomedicine.com/NMIIA.htm).
- [25] J. Fritz et al. Translating biomolecular recognition into nanomechanics. *Science*, 288:316–318, 2000.
- [26] Y. C. Fung. *Biomechanics: Circulation*. Springer, NY, 2nd edition, 1997.
- [27] Aram Galstyan, Tad Hogg, and Kristina Lerman. Modeling and mathematical analysis of swarms of microscopic robots. In P. Arabshahi and A. Martinoli, editors, *Proc. of the IEEE Swarm Intelligence Symposium (SIS2005)*, pages 201–208, 2005.
- [28] V. Gazi and K. M. Passino. Stability analysis of social foraging swarms. *IEEE Trans. on Systems, Man and Cybernetics*, B34:539–557, 2004.
- [29] Shankar Ghosh et al. Carbon nanotube flow sensors. *Science*, 299:1042–1044, 2003.
- [30] Claudia V. Goldman and Shlomo Zilberstein. Optimizing information exchange in cooperative multi-agent systems. In *Proc. of the 2nd Intl. Conf. on Autonomous Agents and Multiagent Systems*, pages 137–144, 2003.
- [31] Tad Hogg and Bernardo A. Huberman. Dynamics of large autonomous computational systems. In Kagan Tumer and David Wolpert, editors, *Collectives and the Design of Complex Systems*, pages 295–315. Springer, New York, 2004.
- [32] Tad Hogg and David W. Sretavan. Controlling tiny multi-scale robots for nerve repair. In *Proc. of the 20th Natl. Conf. on Artificial Intelligence (AAAI2005)*, pages 1286–1291. AAAI Press, 2005.
- [33] Tad Hogg and Kan Zhang. Secure multi-agent communication for microscopic robots. In C. Ortiz, editor, *Proc. of the AAAI Spring Symposium on Bridging the Multi-agent and Multi-robotic Research Gap*, pages 22–26, March 2004.
- [34] Joe Howard. Molecular motors: Structural adaptations to cellular functions. *Nature*, 389:561–567, 1997.

- [35] Nick Jakobi, Phil Husbands, and Inman Harvey. Noise and the reality gap: The use of simulation in evolutionary robotics. In F. Moran et al., editors, *Advances in Artificial Life: Proc. of the 3rd European Conf. on Artificial Life*, pages 704–720. Springer-Verlag, 1995.
- [36] Charles A. Janeway et al. *Immunobiology: The Immune System in Health and Disease*. Garland, 5th edition, 2001.
- [37] George E. M. Karniadakis and Ali Beskok. *Micro Flows: Fundamentals and Simulation*. Springer, Berlin, 2002.
- [38] Kenneth H. Keller. Effect of fluid shear on mass transport in flowing blood. In *Proc. of Federation of American Societies for Experimental Biology*, pages 1591–1599, Sept.-Oct. 1971.
- [39] Balazs L. Keszler, Istvan J. Majoros, and James R. Baker Jr. Molecular engineering in nanotechnology: Structure and composition of multifunctional devices for medical application. In *Proc. of the Ninth Foresight Conference on Molecular Nanotechnology*, 2001.
- [40] Kristina Lerman et al. A macroscopic analytical model of collaboration in distributed robotic systems. *Artificial Life*, 7:375–393, 2001.
- [41] M. Mataric. Minimizing complexity in controlling a mobile robot population. In *Proc. of the 1992 IEEE Intl. Conf. on Robotics and Automation*, pages 830–835, 1992.
- [42] C. William McCurdy et al. Theory and modeling in nanoscience. workshop report, [www.science.doe.gov/bes/reports/files/tmn\\_rpt.pdf](http://www.science.doe.gov/bes/reports/files/tmn_rpt.pdf), US Dept. of Energy, 2002.
- [43] Melissa B. Miller and Bonnie L. Bassler. Quorum sensing in bacteria. *Annual Review of Microbiology*, 55:165–199, 2001.
- [44] Carlo Montemagno and George Bachand. Constructing nanomechanical devices powered by biomolecular motors. *Nanotechnology*, 10:225–231, 1999.
- [45] Kelly Morris. Macrodoctor, come meet the nanodoctors. *The Lancet*, 357:778, March 10 2001.
- [46] NIH. National Institutes of Health roadmap: Nanomedicine, 2003. Available at <http://nihroadmap.nih.gov/nanomedicine/index.asp>.
- [47] Fernando Patolsky and Charles M. Lieber. Nanowire nanosensors. *Materials Today*, 8:20–28, April 2005.
- [48] E. M. Purcell. Life at low Reynolds number. *American Journal of Physics*, 45:3–11, 1977.
- [49] David V. Pynadath and Milind Tambe. Multiagent teamwork: Analyzing the optimality and complexity of key theories and models. In *Proc. of the Intl. Joint Conf. on Autonomous Agents and Multiagent Systems*, pages 873–880, 2002.
- [50] Aristides A. G. Requicha. Nanorobots, NEMS and nanoassembly. *Proceedings of the IEEE*, 91:1922–1933, 2003.
- [51] Ingmar H. Riedel et al. A self-organized vortex array of hydrodynamically entrained sperm cells. *Science*, 309:300–303, 2005.
- [52] B. Salemi, W.-M. Shen, and P. Will. Hormone controlled metamorphic robots. In *Proc. of the Intl. Conf. on Robotics and Automation (ICRA2001)*, 2001.
- [53] Claude E. Shannon and Warren Weaver. *The Mathematical Theory of Communication*. Univ. of Illinois Press, Chicago, 1963.
- [54] Paul E. Sheehan and Lloyd J. Whitman. Detection limits for nanoscale biosensors. *Nano Letters*, 5(4):803–807, 2005.
- [55] Ricky K. Soong et al. Powering an inorganic nanodevice with a biomolecular motor. *Science*, 290:1555–1558, 2000.
- [56] D. Sretavan, W. Chang, C. Keller, and M. Klot. Microscale surgery on axons for nerve injury treatment. *Neurosurgery*, 57(4):635–646, 2005.
- [57] Steven Vogel. *Life in Moving Fluids*. Princeton Univ. Press, 2nd edition, 1994.
- [58] S.-Y. Wang and R. Stanley Williams, editors. *Nanoelectronics*, volume 80. Springer, March 2005. Special issue of *Applied Physics A*.
- [59] Ron Weiss, George E. Homsy, and Thomas F. Knight, Jr. Toward *in vivo* digital circuits. In *Proc. of DIMACS Workshop on Evolution as Computation*, 1999.
- [60] Ron Weiss and Thomas F. Knight, Jr. Engineered communications for microbial robotics. In *Proc. of Sixth Intl. Meeting on DNA Based Computers (DNA6)*, 2000.